THEORETICA CHIMICA ACTA
Theoret. Chim. Acta (Berl.) 62, 319–327 (1983)

Exchange Interactions Between Dimers of Chromium(III). A Cluster Approach

Urs Hauser and Hans U. Güdel

Universität Bern, Institut für anorganische, analytische und physikalische Chemie, Freiestrasse 3, CH-3000 Bern 9, Switzerland

Exchange interactions in dimers, tetramers and octamers of chromium(III) are treated with an effective Hamiltonian of the Heisenberg–Dirac–vanVleck (HDvV) type. Energies and wave functions of the cluster states are computed. The results of interdimer interactions are: (i) energy splittings and (ii) a contamination of the cluster ground state with excited configurations. The results are used for a qualitative rationalisation of the observed low-temperature properties of $Cs_3Cr_2Cl_9$.

Key words: Exchange interactions – Chromium(III) dimer – Chromium(III) tetramer – Chromium(III) octamer.

1. Introduction

Polynuclear complexes of paramagnetic transition metal ions have been intensively studied in the past decade [1]. They serve as molecular model compounds for magnetically ordered materials with extended interactions. In contrast to the latter molecular concepts can be used for the rationalisation of their properties, which makes them attractive to the chemist. Electrostatic interactions between the unpaired electrons on the magnetic centres are formally treated in terms of an effective Hamiltonian, as e.g. the Heisenberg–Dirac–vanVleck (HDvV) Hamiltonian. For a pair of ions it can be written as

$$\mathscr{H}_{ex} = -2J_{ab}(\boldsymbol{S}_a \cdot \boldsymbol{S}_b). \tag{1}$$

J_{ab} is an exchange parameter to be determined by experiment. For a polynuclear complex, i.e. a cluster of paramagnetic ions, exact solutions of the appropriate

Offprint requests to H. U. Güdel.

0040-5744/83/0062/0319/$01.80

HDvV Hamiltonian can usually be obtained. This is in contrast to magnetic Heisenberg systems in which the interaction extends indefinitely in one, two or three dimensions [2]. Solutions can only be approximated in these cases.

In real compounds containing clusters of paramagnetic ions a weak intercluster interaction often occurs in addition to the dominant intracluster coupling. In this situation the molecular picture obviously needs some modification. This can be achieved in two distinctly different ways: (1) by lumping the intercluster effects into a "molecular field" term, the classical procedure in solid state physics, or (2) by explicitly taking intercluster effects into account and constructing a "supercluster" consisting of several clusters in the crystal lattice. This approach may be more appealing to the chemist.

$Cs_3Cr_2Cl_9$ contains $Cr_2Cl_9^{3-}$ dimers with a Cr–Cr distance of 3.19 Å [3]. The intradimer coupling is antiferromagnetic with $-2J \simeq 12\ cm^{-1}$ [4]. Evidence for additional interdimer interactions is provided by inelastic neutron scattering experiments [3]. At temperatures as low as 1.8 K splittings of the "dimer transitions" are observed. For the $S = 0 \rightarrow S = 1$ transition this splitting is of the order of 5 cm^{-1}. In addition the observed transitions show some energy dispersion in $\boldsymbol{k}$ space, a clear indication of their excitonic character. In the present communication we are exploring the possibility of rationalising those observations on the basis of a cluster approach.

2. Theoretical Background

Due to the small single-ion anisotropy exchange interactions in chromium(III) systems can be adequately expressed in terms of a HDvV Hamiltonian. The "supercluster" to be treated is defined in Fig. 1. It is based on the actual

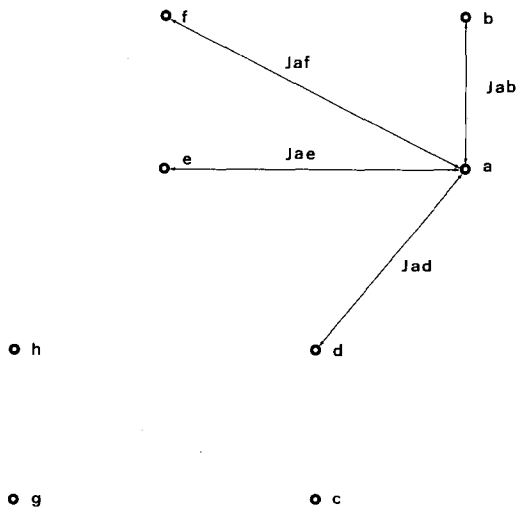

Fig. 1. Definition of the "supercluster" consisting of four identical dimers:

$$J_{ab} = J_{cd} = J_{ef} = J_{gh}; \qquad J_{ad} = J_{de} = J_{eh};$$
$$J_{ae} = J_{bf} = J_{cg} = J_{dh}; \qquad J_{af} = J_{be} = J_{ch} = J_{dg}$$

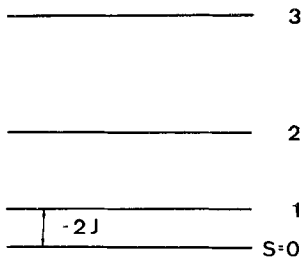

Fig. 2. Dimer energy levels

arrangement of dimers in $Cs_3Cr_2Cl_9$. The energy matrix of the HDvV Hamiltonian is set up and diagonalized for the (a, b) dimer in the first step, the (a, b, c, d) tetramer in the second and the (a, b, c, d, e, f, g, h) octamer in the third step.

The dimer Hamiltonian has been defined in Eq. (1). (1) commutes with the total spin of the pair, and $|S_aS_bSM\rangle$ are the proper pair wave functions, with S taking the values 0, 1, 2, 3. With $S_a = S_b = \frac{3}{2}$ energy eigenvalues are easily obtained as

$$E(S) = 30J_{ab}(-1)^S \begin{Bmatrix} \frac{3}{2} & \frac{3}{2} & 1 \\ \frac{3}{2} & \frac{3}{2} & S \end{Bmatrix} = -J_{ab}[S(S+1) - \tfrac{15}{2}]. \tag{2}$$

The curly bracket in Eq. (2) is a $6-j$ symbol [5]. The corresponding energy level pattern for $J_{ab} = -6\ \mathrm{cm}^{-1}$, an appropriate value for $Cs_3Cr_2Cl_9$, is reproduced in Fig. 2.

For the (a, b, c, d) tetramer the exchange Hamiltonian, neglecting all but nearest-neighbor interactions, is given by

$$\mathscr{H}_{\mathrm{ex}} = -2J_{ab}[(\boldsymbol{S}_a \cdot \boldsymbol{S}_b) + (\boldsymbol{S}_c \cdot \boldsymbol{S}_d)] - 2J_{ad}(\boldsymbol{S}_a \cdot \boldsymbol{S}_d) \tag{3}$$

with the coupling scheme

$$\begin{aligned} \boldsymbol{S}_1 &= \boldsymbol{S}_a + \boldsymbol{S}_b \\ \boldsymbol{S}_2 &= \boldsymbol{S}_c + \boldsymbol{S}_d \\ \boldsymbol{S} &= \boldsymbol{S}_1 + \boldsymbol{S}_2 \end{aligned} \tag{4}$$

the functions

$$|(S_aS_b)S_1(S_cS_d)S_2SM\rangle \tag{5}$$

or briefly

$$|S_1S_2SM\rangle$$

are used as a basis for the energy calculation. Matrix elements are elegantly obtained by applying tensor operator techniques developed and reported by Fano and Racah [6]. They are independent of M, and the 44×44 matrix is

symmetrical:

$$\langle S_1 S_2 S|\mathcal{H}_{ex}|S_1' S_2' S\rangle$$
$$= 30 J_{ab}\delta(S_1 S_1')\delta(S_2 S_2')\left[(-1)^{S_1}\begin{Bmatrix}\frac{3}{2} & \frac{3}{2} & 1\\ \frac{3}{2} & \frac{3}{2} & S_1\end{Bmatrix}+(-1)^{S_2}\begin{Bmatrix}\frac{3}{2} & \frac{3}{2} & 1\\ \frac{3}{2} & \frac{3}{2} & S_2\end{Bmatrix}\right]$$
$$+30\sqrt{(2S_1+1)(2S_1'+1)(2S_2+1)(2S_2'+1)}$$
$$\times\begin{Bmatrix}S_1 & S_1' & 1\\ S_2' & S_2 & S\end{Bmatrix}\begin{Bmatrix}S_1 & S_1' & 1\\ \frac{3}{2} & \frac{3}{2} & \frac{3}{2}\end{Bmatrix}\begin{Bmatrix}S_2 & S_2' & 1\\ \frac{3}{2} & \frac{3}{2} & \frac{3}{2}\end{Bmatrix}(J_{ad}(-1)^{S+1}). \tag{6}$$

Considering only nearest-neighbor interactions the exchange Hamiltonian for the (a, b, c, d, e, f, g, h) octamer is given by

$$\mathcal{H}_{ex} = -2J_{ab}[(\boldsymbol{S}_a\cdot\boldsymbol{S}_b)+(\boldsymbol{S}_c\cdot\boldsymbol{S}_d)+(\boldsymbol{S}_e\cdot\boldsymbol{S}_f)+(\boldsymbol{S}_g\cdot\boldsymbol{S}_h)]$$
$$-2J_{ad}[(\boldsymbol{S}_a\cdot\boldsymbol{S}_d)+(\boldsymbol{S}_d\cdot\boldsymbol{S}_e)+(\boldsymbol{S}_e\cdot\boldsymbol{S}_h)]$$
$$-2J_{ae}[(\boldsymbol{S}_a\cdot\boldsymbol{S}_e)+(\boldsymbol{S}_b\cdot\boldsymbol{S}_f)+(\boldsymbol{S}_c\cdot\boldsymbol{S}_g)+(\boldsymbol{S}_d\cdot\boldsymbol{S}_h)]$$
$$-2J_{af}[(\boldsymbol{S}_a\cdot\boldsymbol{S}_f)+(\boldsymbol{S}_b\cdot\boldsymbol{S}_e)+(\boldsymbol{S}_c\cdot\boldsymbol{S}_h)+(\boldsymbol{S}_d\cdot\boldsymbol{S}_g)]. \tag{7}$$

We choose the coupling scheme

$$\left.\begin{aligned}\boldsymbol{S}_1&=\boldsymbol{S}_a+\boldsymbol{S}_b\\ \boldsymbol{S}_2&=\boldsymbol{S}_c+\boldsymbol{S}_d\\ \boldsymbol{S}_3&=\boldsymbol{S}_e+\boldsymbol{S}_f\\ \boldsymbol{S}_4&=\boldsymbol{S}_g+\boldsymbol{S}_h\end{aligned}\right\}\quad\left.\begin{aligned}\boldsymbol{S}_{12}&=\boldsymbol{S}_1+\boldsymbol{S}_2\\ \boldsymbol{S}_{34}&=\boldsymbol{S}_3+\boldsymbol{S}_4\end{aligned}\right\}\quad \boldsymbol{S}=\boldsymbol{S}_{12}+\boldsymbol{S}_{34}. \tag{8}$$

The corresponding basis functions are thus

$$|\{(S_aS_b)S_1(S_cS_d)S_2\}S_{12}\{(S_eS_f)S_3(S_gS_h)S_4\}S_{34}SM\rangle$$

or briefly

$$|(S_1S_2)S_{12}(S_3S_4)S_{34}SM\rangle. \tag{9}$$

Applying the methods of Fano and Racah [6] expression (10) is obtained for a general matrix element. As in the tetramer case the matrix is symmetrical, and the matrix elements independent of M.

$$\langle\{(S_1S_2)S_{12}(S_3S_4)S_{34}\}S|\mathcal{H}_{ex}|\{(S_1'S_2')S_{12}'(S_3'S_4')S_{34}'\}S\rangle$$
$$= 30J_{ab}\delta(S_1S_1')\delta(S_2S_2')\delta(S_3S_3')\delta(S_4S_4')\delta(S_{12}S_{12}')\delta(S_{34}S_{34}')$$
$$\times\left[(-1)^{S_1}\begin{Bmatrix}\frac{3}{2} & \frac{3}{2} & 1\\ \frac{3}{2} & \frac{3}{2} & S_1\end{Bmatrix}+(-1)^{S_2}\begin{Bmatrix}\frac{3}{2} & \frac{3}{2} & 1\\ \frac{3}{2} & \frac{3}{2} & S_2\end{Bmatrix}\right.$$
$$\left.+(-1)^{S_3}\begin{Bmatrix}\frac{3}{2} & \frac{3}{2} & 1\\ \frac{3}{2} & \frac{3}{2} & S_3\end{Bmatrix}+(-1)^{S_4}\begin{Bmatrix}\frac{3}{2} & \frac{3}{2} & 1\\ \frac{3}{2} & \frac{3}{2} & S_4\end{Bmatrix}\right]$$
$$+30\delta(S_2S_2')\delta(S_4S_4')[(2S_{12}+1)(2S_{12}'+1)(2S_{34}+1)$$
$$\times(2S_{34}'+1)(2S_1+1)(2S_1'+1)(2S_3+1)(2S_3'+1)]^{1/2}$$

$$\times \begin{Bmatrix} S_{12} & S'_{12} & 1 \\ S'_{34} & S_{34} & S \end{Bmatrix} \begin{Bmatrix} S_{12} & S'_{12} & 1 \\ S'_1 & S_1 & S_2 \end{Bmatrix} \begin{Bmatrix} S_1 & S'_1 & 1 \\ \frac{3}{2} & \frac{3}{2} & \frac{3}{2} \end{Bmatrix}$$

$$\times \begin{Bmatrix} S_{34} & S'_{34} & 1 \\ S'_3 & S_3 & S_4 \end{Bmatrix} \begin{Bmatrix} S_3 & S'_3 & 1 \\ \frac{3}{2} & \frac{3}{2} & \frac{3}{2} \end{Bmatrix}$$

$$\times (J_{af}[(-1)^{S_1+S'_1+S_2+S_4+S_{34}+S'_{34}+S+1} + (-1)^{S_2+S_3+S'_3+S_4+S_{34}+S'_{34}+S+1}]$$

$$+ J_{ae}[(-1)^{S_1+S'_1+S_2+S_3+S'_3+S_4+S_{34}+S'_{34}+S+1} + (-1)^{S_2+S_4+S_{34}+S'_{34}+S+1}])$$

$$+ 30\delta(S_1S'_1)\delta(S_3S'_3)[(2S_{12}+1)(2S'_{12}+1)(2S_{34}+1)$$

$$\times (2S'_{34}+1)(2S_2+1)(2S'_2+1)(2S_4+1)(2S'_4+1)]^{1/2}$$

$$\times \begin{Bmatrix} S_{12} & S'_{12} & 1 \\ S'_{34} & S_{34} & S \end{Bmatrix} \begin{Bmatrix} S_{12} & S'_{12} & 1 \\ S'_2 & S_2 & S_1 \end{Bmatrix} \begin{Bmatrix} S_2 & S'_2 & 1 \\ \frac{3}{2} & \frac{3}{2} & \frac{3}{2} \end{Bmatrix}$$

$$\times \begin{Bmatrix} S_{34} & S'_{34} & 1 \\ S'_4 & S_4 & S_3 \end{Bmatrix} \begin{Bmatrix} S_4 & S'_4 & 1 \\ \frac{3}{2} & \frac{3}{2} & \frac{3}{2} \end{Bmatrix}$$

$$\times (J_{af}[(-1)^{S_1+S_3+S_4+S'_4+S_{12}+S'_{12}+S+1} + (-1)^{S_1+S_2+S'_2+S_3+S_{12}+S'_{12}+S+1}]$$

$$+ J_{ae}[(-1)^{S_1+S_3+S_{12}+S'_{12}+S+1} + (-1)^{S_1+S_2+S'_2+S_3+S_4+S'_4+S_{12}+S'_{12}+S+1}])$$

$$+ 30J_{ad}\Big(\delta(S_{12}S'_{12})\delta(S_{34}S'_{34})\Big[\delta(S_3S'_3)\delta(S_4S'_4)(-1)^{S_{12}+1}$$

$$\times [(2S_1+1)(2S'_1+1)(2S_2+1)(2S'_2+1)]^{1/2}$$

$$\times \begin{Bmatrix} S_1 & S'_1 & 1 \\ S'_2 & S_2 & S_{12} \end{Bmatrix} \begin{Bmatrix} S_1 & S'_1 & 1 \\ \frac{3}{2} & \frac{3}{2} & \frac{3}{2} \end{Bmatrix} \begin{Bmatrix} S_2 & S'_2 & 1 \\ \frac{3}{2} & \frac{3}{2} & \frac{3}{2} \end{Bmatrix} + \delta(S_1S'_1)\delta(S_2S'_2)(-1)^{S_{34}+1}$$

$$\times [(2S_3+1)(2S'_3+1)(2S_4+1)(2S'_4+1)]^{1/2}$$

$$\times \begin{Bmatrix} S_3 & S'_3 & 1 \\ S'_4 & S_4 & S_{34} \end{Bmatrix} \begin{Bmatrix} S_3 & S'_3 & 1 \\ \frac{3}{2} & \frac{3}{2} & \frac{3}{2} \end{Bmatrix} \begin{Bmatrix} S_4 & S'_4 & 1 \\ \frac{3}{2} & \frac{3}{2} & \frac{3}{2} \end{Bmatrix}\Big]$$

$$+ \delta(S_1S'_1)\delta(S_4S'_4)(-1)^{S_1+S_2+S'_2+S_3+S'_3+S_4+S_{12}+S'_{12}+S_{34}+S'_{34}+S+1}$$

$$\times [(2S_2+1)(2S'_2+1)(2S_3+1)(2S'_3+1)$$

$$\times (2S_{12}+1)(2S'_{12}+1)(2S_{34}+1)(2S'_{34}+1)]^{1/2}$$

$$\times \begin{Bmatrix} S_{12} & S'_{12} & 1 \\ S'_{34} & S_{34} & S \end{Bmatrix} \begin{Bmatrix} S_{12} & S'_{12} & 1 \\ S'_2 & S_2 & S_1 \end{Bmatrix} \begin{Bmatrix} S_{34} & S'_{34} & 1 \\ S'_3 & S_3 & S_4 \end{Bmatrix}$$

$$\times \begin{Bmatrix} S_2 & S'_2 & 1 \\ \frac{3}{2} & \frac{3}{2} & \frac{3}{2} \end{Bmatrix} \begin{Bmatrix} S_3 & S'_3 & 1 \\ \frac{3}{2} & \frac{3}{2} & \frac{3}{2} \end{Bmatrix}\Big). \tag{10}$$

3. Computational Procedure

All the computations were carried out on the IBM 370/158 machine of the computer centre of the university of Bern. Programs were written for the

calculation of matrix elements. The real symmetrical matrices were diagonalized by the use of the following routines: EIGEN (Scientific Subroutine Package) for the tetramer; F02ABF (Numerical Algorithms Group routine) for the octamer. EIGEN is based on the Jacobi diagonalisation procedure [7], whereas F02ABF converts the real symmetrical matrix into tridiagonal form by the householder method in a first step and then computes eigenvalues and eigenvectors using the *QL* algorithm [8]. The matrix (10) is blockdiagonal with one block for each value of S. We were only interested in the blocks with $S = 0$ (dimension 364), $S = 1$ (dimension 1000) and $S = 2$ (dimension 1400). For economic reasons the $S = 1$ and 2 blocks were diagonalized by an approximate method. Each block can be arranged as a matrix with non-zero elements on a band along the diagonal. Diagonalizing only the part with S_1, S_2, S_{12}, S_3, S_4, $S_{34} \leq 2$ of the full matrix proved to be accurate in our case.

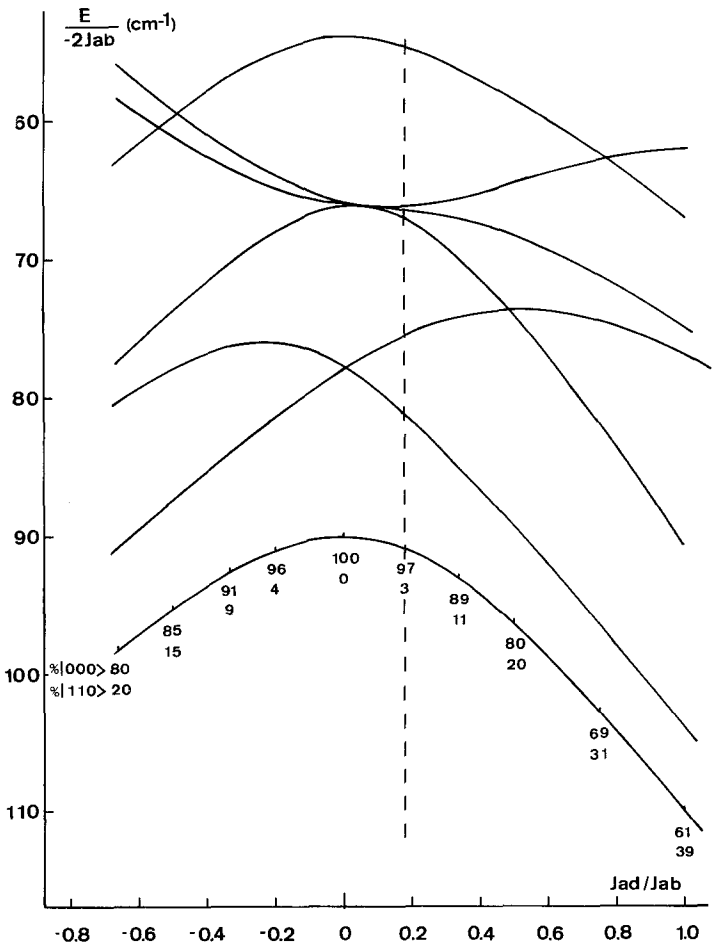

Fig. 3. Correlation diagram for the lowest-energy tetramer (*a*, *b*, *c*, *d*) states as a function of the ratio of inter to intradimer exchange. The mixing coefficients of the groundstate wave function are included

4. Results and Discussion

The dimer energy splitting (Fig. 2) is a simple Landé pattern. As a result of the antiferromagnetic coupling the dimer ground state is $S = 0$.

In Fig. 3 the energies of the lowest tetramer states are plotted as a function of J_{ad}/J_{ab}, i.e. the inter to intradimer exchange. $|(S_aS_b)S_1(S_cS_d)S_2S\rangle$ are proper tetramer functions only for $J_{ad}/J_{ab} = 0$. Off-diagonal matrix elements between functions with $\Delta S = 0$, ΔS_1 and $\Delta S_2 = 0, \pm 1$ lead to the observed mixing for non-zero J_{ad} values. Our particular interest is in the cluster ground state, because it determines the magnetic properties at the lowest temperatures. In the absence of interdimer exchange the tetramer ground state is $|000\rangle$, i.e. both contributing dimers are in their respective ground states. With increasing $|J_{ad}|$ $|110\rangle$ is increasingly mixed into the ground state wave function. The mixing coefficients are included in Fig. 3. $|110\rangle$ corresponds to a configuration in which the dimers, both in their first excited state $S = 1$, couple antiferromagnetically. Splittings of the $S = 1$ dimer level of the order of the experimentally observed energy separations are obtained for $J_{ad}/J_{ab} \cong 1/6$ (dashed line in Fig. 3). The $|110\rangle$ contribution to the tetramer ground state is 3% at this J_{ad}/J_{ab} ratio.

For the octamer computations all the three interdimer exchange parameters J_{ad}, J_{ae}, J_{af} were set equal $-1\ \mathrm{cm}^{-1}$, corresponding to ratios of inter to intradimer exchange of 1/6. The corresponding interdimer Cr–Cr distances in $Cs_3Cr_2Cl_9$ are all lying in the range 7–8 Å [9]. Fig. 4 shows a comparison of energy splittings for a dimer, tetramer and octamer. It illustrates the high density of octamer states above $20\ \mathrm{cm}^{-1}$. A total of 8092 octamer states arise out of the 44 tetramer states as a result of the additional intertetramer couplings. In the low-energy part the octamer ground state is the only one separated from neighboring states by more than $8\ \mathrm{cm}^{-1}$. This is also reflected by the wave functions. Excited cluster states are highly mixed, and a predominant $|(S_1S_2)S_{12}(S_3S_4)S_{34}S\rangle$ contribution is not discernible. The ground state, however, is still predominantly $|000\ 000\ 0\rangle$.

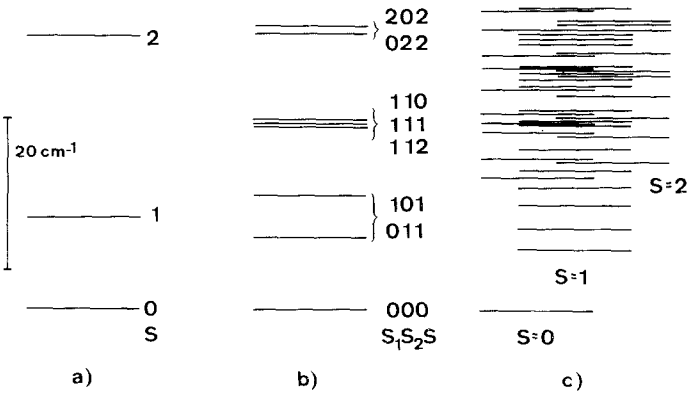

Fig. 4a–c. Low-energy part of the splitting pattern for **a)** dimer (a, b); **b)** tetramer (a, b, c, d); **c)** octamer as defined in Fig. 1. $J_{ab} = -6\ \mathrm{cm}^{-1}$, $J_{ad} = J_{ae} = J_{af} = -1\ \mathrm{cm}^{-1}$

$|000\ 110\ 0\rangle$, $|110\ 000\ 0\rangle$ and $|011\ 101\ 0\rangle$ contribute 3% each. This demonstrates that the contamination of the cluster ground state with configurations in which individual dimers are in their $S = 1$ excited states increases with increasing size of the cluster. In the tetramer this contribution from excited configurations is 3%, whereas in the octamer it is 9%. Without performing explicit calculations we can predict that this increase will continue until all the nearest neighbors of a given dimer have been taken into account. In $Cs_3Cr_2Cl_9$ the number of neighbors within the 7–8 Å range is 12 [9]. In our octamer model only three of these are considered.

5. Conclusions

Energy splittings of the "dimer states", observed by inelastic neutron scattering in $Cs_3Cr_2Cl_9$, can qualitatively be rationalized in terms of simple cluster models. A ratio of inter to intradimer exchange of the order of 1/6 appears reasonable in comparison with corresponding values in low-dimensional halide systems [2]. Of the large number of octamer states arising from the dimer $S = 1$ state only very few are accessible by inelastic neutron scattering from the ground state in good qualitative agreement with the observed scattering behavior [3].

Energy dispersion in $\boldsymbol{k}$ space is a solid state phenomenon. As such it can only be properly treated by theories taking explicit account of the translational symmetry of the crystal lattice. Our cluster approach, nevertheless, provides some valuable insight into the physical origin of the cooperative effects. The ground configurations $|000\rangle$ (tetramer) and $|000\ 000\ 0\rangle$ (octamer) in which all the contributing dimers are in their $S = 0$ ground states, cannot provide a mechanism for any extended interactions. These configurations make up the cluster ground state in the absence of interdimer exchange. They are still the dominant contributions to the ground state for realistic values of J interdimer/J intradimer. But configurations in which nearest-neighbor dimers are excited to their $S = 1$ state also contribute to the cluster ground state. And from our calculations we can safely conclude that this will also be true for very large clusters. This contribution of excited configurations to the cluster ground state provides a basis for the extended interactions which result in the observed cooperative effects at the lowest temperatures [3].

Acknowledgment. This work was supported by the Swiss National Science Foundation (Grant No. 2.673-080).

References

1. Carlin, R. L., van Duyneveldt, A. J.: Magnetic properties of transition metal compounds, p. 77 New York: Springer Verlag, 1977
2. de Jongh, L. J., Miedema, A. R.: Adv. Phys. **23**, 1 (1974)
3. (a) Stebler, A., Güdel, H. U., Furrer, A., Kjems, J.: J. Appl. Phys. **53**, 1996 (1982)
   (b) Stebler, A.: Dissertation, University of Bern, 1981

4. Kahn, O., Briat, B.: Chem. Phys. Letters **32**, 376 (1975)
5. Rotenberg, M., Bivins, R., Metropolis, N., Wooten, J. K.: The 3-*j* and 6-*j* symbols. The Technology Press MIT, 1959
6. Fano, U., Racah, G.: Irreducible tensorial sets. New York: Academic Press, 1959
7. Ralsten, A., Wilf, H. F.: Mathematical methods for digital computers, Chapter 7. New York: John Wiley and Sons, 1962
8. Wilkinson, J. H., Reinsch, C.: Linear algebra, New York: Springer Verlag, 1971
9. Wessel, G. J., Ijdo, D. J. W.: Acta Cryst. **10**, 466 (1957)

Received August 5, 1982